Interplay of monopoles and chiral symmetry breaking in noncompact lattice QED

John B. Kogut
Department of Physics, University of Illinois at Urbana-Champaign, 1110 West Green Street, Urbana, Illinois 61801-3080

K. C. Wang
School of Physics, University of New South Wales, P.O. Box 1, Kensington, New South Wales 2203, Australia
(Received 18 January 1995)

Noncompact lattice QED is simulated for various numbers of fermion species N_f ranging from 8 through 40 by the exact hybrid Monte Carlo algorithm. Over this range of N_f, chiral symmetry breaking is found to be strongly correlated with the effective monopoles in the theory. For N_f between 8 and 16, the chiral symmetry breaking and monopole percolation transitions are second order and coincident. Assuming power law critical behavior, the correlation length exponent for the chiral transition is identical to that of monopole percolation. This result supports the conjecture that monopole percolation "drives" the nontrivial chiral transition. For N_f between 20 and 32, the monopoles experience a first-order condensation transition coincident with a first-order chiral transition. For N_f as large as 40, both transitions are strongly suppressed. The data at large $N_f (N_f \gtrsim 20)$ are interpreted in terms of a strongly interacting monopole gas-liquid transition.

PACS number(s): 11.15.Ha, 11.30.Rd

I. INTRODUCTION

The interplay of monopole and fermion dynamics has been studied both analytically and computationally in quantum field theory for some time. In the context of grand unified model building, the existence of monopole solutions of the field equations and the subsequent interactions of the monopole with the theory's fermions has led to several interesting phenomena including the existence of exotic fermion condensates and the Callan-Rubakov effect [1]. The Dirac condition plays a crucial role in these discussions and in some cases it guarantees that qualitatively new, nonperturbative effects occur.

It is, therefore, of some interest when monopoles play a role in a broader context. In particular, various models studied in lattice gauge theory afford new glimpses into monopole physics, since the *second quantized* field theory of monopoles becomes accessible. A classic example is the confinement-deconfinement transition in Abelian lattice gauge theory which is now understood to be driven by monopole condensation [2]. It came as some surprise, however, when effective monopoles were discovered in noncompact lattice QED [3], and the percolation transition of these objects was seen to be the same as four-dimensional bond percolation [4]. The lattice itself allows such objects to have finite action, but one would expect naively that they would decouple in the theory's continuum limit. But this depends on the scaling properties of the monopole percolation transition. When noncompact lattice QED is coupled to fermions in the traditional, explicitly gauge-invariant fashion of Schwinger [through U(1) phases] one finds that the monopole percolation and the chiral symmetry transitions are coincident [5]. Even more tantalizing is the fact that the correlation length exponents for both transitions also coincide, so monopoles could survive the continuum limit of the chiral transition and the chiral transition itself may represent an interacting continuum field theory in four dimensions. Needless to say, it will prove extraordinarily hard to establish such a scenario purely numerically [6].

It is the purpose of this paper to elucidate the interplay of monopole and fermion dynamics in noncompact lattice QED by studying the system's phase transitions as N_f, the number of fermion species, is varied. Since the fermion-monopole interaction strength is determined by the Dirac quantization condition, N_f is the only natural variable available. We are not in a position to make a quantitative study of each theory's continuum limit. All our results will be of a semiquantitative or even qualitative sort. We think that they are interesting and have content, nonetheless. Our lattice sizes will be modest (typically 10^4) as will our bare fermion masses (typically of order 0.05 and greater in lattice units). It turned out that finite size effects are particularly large when N_f is large so that smaller bare fermion masses cannot be sensibly studied on 10^4 lattices. This fact will also force our chiral symmetry-breaking studies to be done rather far from the chiral limit, and therefore they are not as quantitative as one might hope.

Since this paper continues a large body of work discussed in detail elsewhere, it will rely on definitions and formulas already presented [3–5]. The reader should consult those references for background. Quantities such as the chiral condensate $\langle\overline{\psi}\psi\rangle$, the monopole susceptibility χ, and the monopole percolation order parameter M should be familiar and will not be reviewed here. Equation of state, scaling laws, and critical indices should also be familiar to the reader. Our notation will be the same as past publications.

One of the goals of the present investigation is a better understanding of the physical significance of effective

monopoles in noncompact QED. Since the gauge field piece of the action is purely Gaussian, it is surprising that effective monopoles can have any significance at all. However, they are detected in gauge field configurations using the same operators invented to detect monopoles in pure compact U(1) theory [7], and they couple to fermions through U(1) phases. In the quenched limit, however, the monopoles do not interact among themselves (since the gauge field piece of the action is Gaussian) and their transition is well described by percolation, a counting problem. Nonetheless, there is the intriguing possibility that the percolation transition can induce nontrivial dynamics in the fermion sector in unquenched models if the two transitions coincide. We shall see that this perspective has support from our simulations. The reader should note, however, that the simulation data obtained here can be used to test other scenarios describing chiral symmetry breaking in noncompact QED, and we hope that our extensive tables of measurements for various N_f will inspire such efforts. A crucial point in our work is that in models with different bare parameters, such as N_f, where the chiral and monopole percolation transitions are coincident and second order, the chiral critical indices should be the same. It is not clear that this result on critical indices is easy to obtain in other scenarios.

We shall see in the body of this paper that varying N_f over a wide range leaves the chiral and monopole percolation transitions coincident within uncertainties. In these cases it is reasonable to investigate the possibility that the two transitions are intimately related and share several aspects of their critical behavior. The coincidence of the two transitions is certainly dependent on the form of the lattice action used here. Recent work by Hands and one of the authors has demonstrated this in the context of quenched models with generalized actions [8]. In these toy models the relative positions of the two transitions could be changed by altering the bare action and effectively changing the relative importance of long-range photon exchange and short-range attraction. It would be particularly interesting to generalize this study to unquenched models.

We begin with an overview of our results. For N_f equal 2 and 4, we will rely on past, more quantitative studies [5]. The $N_f = 8$ and 16 simulations were done on 10^4 lattices, with selected simulations on $12^4, 14^4$, and 16^4 lattices to check for finite size effects. Accurate studies of the chiral condensate showed that only bare fermion masses greater or equal to 0.05 (in lattice units) are free of finite size effects. This result implies that some past studies of lattice QED at large N_f were not under quantitative control [9]. Data taken at bare fermion masses of 0.05, 0.06, 0.07, 0.08, 0.09, and 0.10, and at couplings ranging from $\beta = 0.21$ to 0.14 in steps of $\Delta\beta = 0.005$, are consistent with the hypothesis that there is a chiral transition at $\beta_c = 0.17(1)$ with power law critical singularities. The critical indices for the chiral transition are consistent with those measured more precisely for the $N_f = 2$ and 4 theories previously. Measurements of the monopole percolation observables also indicate a second order phase transition at essentially the same coupling, $\beta_m = 0.180(5)$, with critical indices characteristic of conventional four-dimensional bond (or site) percolation. The coincidence of the chiral and monopole percolation transitions has been noted before in the $N_f = 2$ and 4 theories [5]. Even more intriguing than this is the fact that both transitions may share the same correlation length index ν. Precise measurements of monopole percolation in four dimensions have strongly suggested the exact result $\nu = \frac{2}{3}$ [4]. Measurements of the chiral equation of state presented here for $N_f = 8$ and elsewhere for $N_f = 2$ and 4 give the critical indices $\delta = 2.2(1)$ and $\gamma = 1.0(1)$. If we assume that the critical point has power law singularities with conventional properties, then the critical indices should satisfy the hyperscaling relations, and δ and γ determine all of them. The hyperscaling relations read

$$\begin{aligned} 2 - \alpha &= d\nu, \\ 2\beta_{\rm mag}\delta - \gamma &= d\nu, \\ \beta_{\rm mag} &= \frac{\nu}{2}(d - 2 + \eta), \\ 2\beta_{\rm mag} + \gamma &= d\nu. \end{aligned} \tag{1.1}$$

Then the values $\delta = 2.2$ and $\gamma = 1$ imply $\beta_{\rm mag} = 0.83, \nu = 0.67, \alpha = -0.67, \eta = 0.50$, and $\Delta \equiv \beta_{\rm mag}\delta = 1.83$. The intriguing result of this exercise is that measurements of the chiral exponents and the hypothesis of hyperscaling predict that the correlation length exponents ν of both transitions are identical. This implies that the monopoles are relevant degrees of freedom at the chiral transition and since they scale identically, the monopoles should survive in the continuum limit of the chiral transition. It might be accurate to say that monopole percolation "drives" the chiral transition and the chiral transition defines an interacting, continuum field theory because it "inherits" the nonmean-field correlation length critical index $\nu = \frac{2}{3}$ from monopole percolation. We shall see in the text through analysis of our measurements of the order parameter $\langle\overline{\psi}\psi\rangle$ that this interpretation fits the computer simulation data very well. However, other hypotheses, such as the possibility that the chiral transition is described by a logarithmically trivial Nambu–Jona-Lasinio model, might fit the data adequately as well. It would require considerably more computer power to separate the monopole picture of the transition from other possibilities just on the basis of numerical fits. One reason for this difficulty is the fact that finite size effects grow large as N_f increases and small bare fermion masses close to the chiral limit cannot be simulated on lattices of practical proportions like 10^4 or even 16^4. For this reason the emphasis in this paper will be different, although elsewhere the $N_f = 2$ and 4 models are being simulated on even larger lattices with even better statistics.

We consider the $N_f = 12, 16, 20, 24, 32$, and 40 models here, and measure $\langle\overline{\psi}\psi\rangle$ and monopole observables to see if the correlation between these observables persists at all N_f. We shall see that while the character of the transitions changes qualitatively as N_f increases, the two transitions remain strongly correlated. To avoid finite size effects we were forced to simulate a relatively large

bare fermion mass $m = 0.10$ on 10^4 lattices. Therefore, many of our conclusions are just qualitative. Luckily, qualitative changes were seen in the data as N_f varied so the study remained useful. We found that as N_f was increased from 8 to 24, the chiral and monopole percolation transitions both shifted to stronger critical couplings but they remained coincident and apparently second order. However, at $N_f \approx 24$ and $m = 0.10$, both transitions displayed jumps suggesting first-order behavior. (The reader should be careful not to overlook our caveats expressed above in these remarks—simulations at smaller m and larger lattices are really necessary to make such statements.) At $N_f = 24$, the chiral condensate $\langle\bar{\psi}\psi\rangle$ and the monopole percolation order parameter M display "discontinuous" jumps between couplings $\beta = 0.08$ and 0.085. Increasing N_f even further to 32 simply enhances the sizes of the apparent discontinuities. The fact that the character of the transition for N_f between 8 and 24 is different from that for N_f between 24 and 40 is supported by measurements of the monopole concentration (density). For small N_f, where the monopole transition is percolation, the concentration of monopoles is expected to be small and smooth through the transition. The simulations show this clearly. However, our simulations at $N_f = 24$ and especially $N_f = 32$ show that the concentration jumps "discontinuously" at the chiral transition, strongly suggesting a first-order transition between a dilute "gaseous state" of monopoles and a fairly dense "liquid" state. For example, at $N_f = 32$ the monopole concentration jumps from $\sim$0.10 at $\beta = 0.055$ to 0.34 at $\beta = 0.050$. Since the transition shows up in the monopole concentration, it is accurate to call it a "condensation" transition. Since c = 0.34 is a substantial density (the maximal value of c is slightly under one-half), it is very tantalizing to view the transition as a first-order gas-liquid transition. Apparently increasing N_f affects the monopole core energy and/or the monopole-monopole interactions and thereby induces a gas-liquid transition. It would be interesting to complement the computer results with some analytic calculations.

Of course this physical picture of the transition needs further substantiation. One element of it that we could test here was the expectation that if fermion-induced forces were affecting the monopole dynamics and leading to a gas-liquid transition, then if N_f were taken truly large, free monopoles would never appear in the system. In fact, we confirmed this point at $N_f = 40$. The simulation showed that the monopole concentration and the monopole percolation susceptibility and the monopole percolation order parameter all remained strongly suppressed and flat as the coupling varied. The chiral condensate was similarly suppressed. However, the plaquette showed strong dependence on the coupling β suggesting that a transition remains in the model with a divergent specific heat, but it is unrelated to the monopole or chiral properties of the model. The small values of M and c indicate that the monopoles remain bound in tight pairs for all coupling β. Under these circumstances one would not expect them to induce chiral symmetry breaking and our simulations are consistent with that fact.

The phase diagram (N_f vs β) that we are advocating here agrees qualitatively with that of Azcoiti and collaborators [10]. Their work emphasizes the theory's specific heat, while ours emphasizes monopole and chiral dynamics. We believe that these are two views of the same physics, and the qualitative features we are interested in and can deal with fairly reliably, are identical.

The body of this paper is organized as follows. In Sec. II the $N_f = 8$ theory is discussed in detail. In Sec. III we turn to the $N_f = 12, 16, 20$, and 24 data, and show that the $N_f = 24$ data displays monopole condensation. In Sec. IV we turn to the $N_f = 32$ and 40 data which show that for truly large N_f the monopole and chiral activities in the theory are strongly suppressed.

II. THE $N_f = 8$ SIMULATION

We used our hybrid Monte Carlo code for noncompact QED to explore the eight flavor, $N_f = 8$, model just as we studied the $N_f = 4$ case more quantitatively in an earlier publication. The reader should consult our extensive $N_f = 2$ and 4 studies for details of the algorithm and the definitions of various chiral and monopole observables [3–5]. Since this paper is looking for qualitative trends

TABLE I. Chiral condensate, $N_f = 8$, $L = 10$.

β/m	0.03	0.04	0.05	0.06	0.07	0.08	0.09	0.10
0.200	0.1066(5)	0.1396(7)	0.1677(7)	0.1947(6)	0.2148(7)	0.2368(8)	0.2545(7)	0.2739(7)
0.195	0.1139(7)	0.1468(9)	0.1778(8)	0.2056(7)	0.2270(8)	0.249(1)	0.269(1)	0.2835(7)
0.19	0.1246(6)	0.160(1)	0.1903(8)	0.2160(7)	0.2388(8)	0.260(1)	0.280(1)	0.2958(7)
0.185	0.1370(7)	0.173(1)	0.2036(8)	0.2290(8)	0.252(1)	0.274(1)	0.293(1)	0.3098(8)
0.18	0.147(1)	0.188(1)	0.2179(8)	0.247(1)	0.268(1)	0.288(1)	0.305(1)	0.3232(8)
0.175	0.167(1)	0.209(1)	0.236(1)	0.261(1)	0.286(1)	0.304(1)	0.319(1)	0.3364(9)
0.17	0.181(1)	0.219(1)	0.256(1)	0.279(1)	0.302(1)	0.321(1)	0.335(1)	0.352(1)
0.165	0.203(1)	0.242(1)	0.274(1)	0.300(1)	0.322(1)	0.335(1)	0.353(1)	0.369(1)
0.16	0.232(1)	0.265(1)	0.297(1)	0.320(1)	0.340(1)	0.358(1)	0.371(1)	0.382(1)
0.155	0.262(1)	0.293(1)	0.323(1)	0.341(1)	0.360(1)	0.377(1)	0.386(1)	0.399(1)
0.15	0.291(2)	0.319(1)	0.344(1)	0.364(1)	0.380(1)	0.394(1)	0.407(1)	0.417(1)
0.145	0.324(2)	0.349(1)	0.371(1)	0.386(1)	0.405(1)	0.416(1)	0.425(1)	0.434(1)
0.14	0.355(2)	0.377(1)	0.398(1)	0.412(1)	0.424(1)	0.435(1)	0.444(1)	0.452(1)

TABLE II. Chiral condensate, $N_f = 8, L = 12$.

β/m	0.03	0.05
0.200	0.1123(5)	0.1723(8)
0.190	0.1280(8)	0.1916(8)
0.185	0.1388(7)	0.2030(6)
0.180	0.1516(7)	0.2185(6)
0.175	0.1657(7)	0.2344(8)
0.170	0.1824(8)	0.2520(7)
0.160	0.229(1)	0.2949(9)
0.150	0.289(1)	0.345(1)
0.140	0.355(1)	0.396(1)

and is a contribution in a long series, we will not repeat formulas, definitions, and past observations. Rather, our emphasis will be on results, plots, and an emerging physical picture.

To gain some understanding of the chiral transition at $m = 0.0$ we measured $\langle\bar{\psi}\psi\rangle$ for bare fermion masses ranging from 0.03 to 0.10 and couplings $\beta = 1/e^2$ ranging from 0.20 to 0.14. The data are shown in Table I. Several hundred trajectories of the hybrid Monte Carlo code were required to achieve the statistical accuracy indicated in the table. Since the lattice size is relatively small, 10^4, we must be careful about finite size effects in the data, especially at small values of m. Therefore, we did limited simulations on $12^4, 14^4$, and 16^4 lattices. The data is shown in Tables II–IV. Comparing Tables I and II, we see evidence on the weak coupling side of the chiral transition, $\beta = 0.20$–0.18, for numerically significant finite size effects for the lowest fermion mass, $m = 0.03$. Over this range of parameters, $\langle\bar{\psi}\psi\rangle$ is relatively suppressed on the smaller lattice, which is the expected finite size/finite temperature effect. However, comparing Tables I–IV we see that the finite size effects are within our statistical error bars at $m = 0.05$, except perhaps at the weakest coupling $\beta = 0.200$. Therefore, in the analysis that follows only the 10^4 data for m ranging from 0.05 to 0.10 will be used.

We will assume that the chiral transition is well-described by a second order phase transition with power law singularities. Other hypotheses could be tried here and some would probably be fairly successful since our data covers only relatively large m values and every fitting hypothesis is accompanied by several free parameters. We will pursue the power law hypothesis here because it is simple and because it is definitely appropriate for monopole percolation [4]. Given this, the data should satisfy the equation of state (EOS)

TABLE III. Chiral condensate, $N_f = 8, L = 14$.

β/m	0.05
0.185	0.2032(4)
0.180	0.2188(4)
0.170	0.2356(5)

TABLE IV. Chiral condensate, $N_f = 8, L = 16$.

β/m	0.05
0.185	0.2043(3)
0.180	0.2184(3)
0.170	0.2340(4)

$$\langle\bar{\psi}\psi\rangle/m^{\frac{1}{\delta}} = f(\Delta\beta/\langle\bar{\psi}\psi\rangle^{\frac{1}{\beta_{\rm mag}}}), \tag{2.1}$$

where δ and $\beta_{\rm mag}$ are the usual critical indices and $\Delta\beta = \beta_c - \beta$, and this form of the EOS has been used extensively elsewhere. Equation (2.1) simplifies at the critical point and reduces to the scaling law of the order parameter $\langle\bar{\psi}\psi\rangle$ as the symmetry-breaking field m is turned on:

$$\langle\bar{\psi}\psi\rangle = Am^{\frac{1}{\delta}}, \quad \beta = \beta_c. \tag{2.2}$$

We found that Eq. (2.2) is a particularly effective way to determine δ and β_c which then can be used in the EOS to find the universal scaling function f and the critical index $\beta_{\rm mag}$ away from the transition. In Fig. 1 we plot $-1/\ln\langle\bar{\psi}\psi\rangle$ vs $-1/\ln(m)$ for the data of Table I ($m \geq 0.05$). For infinitesimal m and $\langle\bar{\psi}\psi\rangle$, these lines should be straight with the slope $\frac{1}{\delta}$ at $\beta = \beta_c$, and they should pass through the origin. We see that this hypothesis works well at $\beta_c = 0.17$ in Fig. 1 for $m = 0.05$–0.10. The lower masses are subject to finite size effects, as discussed above, and must be discarded. The slope of the $\beta_c = 0.17$ line in Fig. 1 gives $\delta = 2.2(1)$. Power law fits of the $\beta = 0.17$ data to Eq. (2.2) are excellent indicating that the numerical evidence for the power law hypothesis is perfectly consistent with the numerical data. Such fits produce estimates of the constant A in Eq. (2.2). A is predicted to be very close to one, so that it does not affect the curves and δ estimate in Fig. 1. (The reader can verify that A is consistent with unity by reading the vertical axis of Fig. 2 when β is set to β_c, zero on the horizontal axis.) One can also estimate β_c and δ by plot-

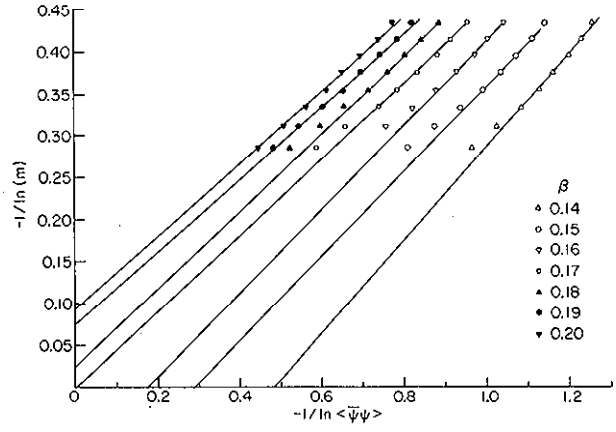

FIG. 1. $-1/\ln(m)$ vs $-1/\ln\langle\bar{\psi}\psi\rangle$ plot showing critical behavior at $\beta = 0.17$.

ting $\ln\langle\bar{\psi}\psi\rangle$ vs $\ln(m)$ and looking for the best linear fit for various β. This method, which is independent of the constant A and was used in the $N_f = 2$ and 4 cases also, produces $\beta_c = 0.17$ and $\delta = 2.23(14)$.

We also took the data in Table I and fit them to the simple EOS

$$m = C\langle\bar{\psi}\psi\rangle^{\delta} + B(\beta - \beta_c)\langle\bar{\psi}\psi\rangle. \tag{2.3}$$

Using the $m = 0.05, 0.06, 0.07$, and 0.08 data, a stable fit was found and the parameters $\delta = 2.30(16)$, $\beta_c = 0.164(4)$, $C = 0.935(76)$, and $B = 5.90(19)$ were predicted. These results are consistent with the results obtained above by more elementary, transparent methods. We did not use the lower mass data ($m = 0.03$ and 0.04) in this fit because of the finite size effects discussed above. Neither did we use the higher mass data ($m = 0.09$ and 0.10) because they lie outside the scaling region, as one can observe visually in Fig. 1.

We note that the result $\delta = 2.2(1)$ is consistent with the results found at $N_f = 2$ and 4, assuming power law singularities at the critical point. Those data also gave the susceptibility index $\gamma = 1.0(1)$ which, by the hyperscaling relation $\beta_{\rm mag} = \gamma/(\delta - 1)$, predicted $\beta_{\rm mag} = 0.83(7)$, the magnetic critical index. This motivated us to try the EOS equation (2.1) with $\beta_{\rm mag} = 0.83$. The result is shown in Fig. 2. The data fall on a universal scaling function f rather well, although the quality of the data and the resulting universal curve are not comparable to our $N_f = 2$ and 4 results which came from larger lattices and smaller values of m. However, if we compare the EOS for $N_f = 8$ in Fig. 2 to the analogous figures in the $N_f = 2$ and 4 publications, we see that even the universal function f as well as the critical indices δ and $\beta_{\rm mag}$ are consistent in their independence of N_f. One interpretation of this result is that monopole percolation drives each transition, as discussed in the introduction above, and fermion feedback does not affect the percolation critical behavior as long as N_f is not too large. More evidence for this scenario will be presented below when monopole observables are presented and analyzed. There is no doubt, however, that other more mundane explanations of these systematics could be presented. For example, it could be that all the $N_f \neq 0$ theories are logarithmically trivial and have the scaling properties of Nambu–Jona-Lasinio (NJL) models. If this hypothesis is true, the reason for the deviation of δ and $\beta_{\rm mag}$ from their mean-field values of 3 and 1/2, respectively, is the presence of scale-breaking logarithms in the NJL equation of state. The limited accuracy of our $N_f = 8$ makes it pointless to pursue alternative fits here—given a few new parameters as would occur in NJL fits, this could certainly be done. Rather, we shall investigate just qualitative features of the models with higher N_f and accumulate additional evidence for strong correlations between the chiral and monopole activities in each model. This will then provide "supporting, circumstantial evidence" for the monopole-driven chiral transition physical picture we are developing.

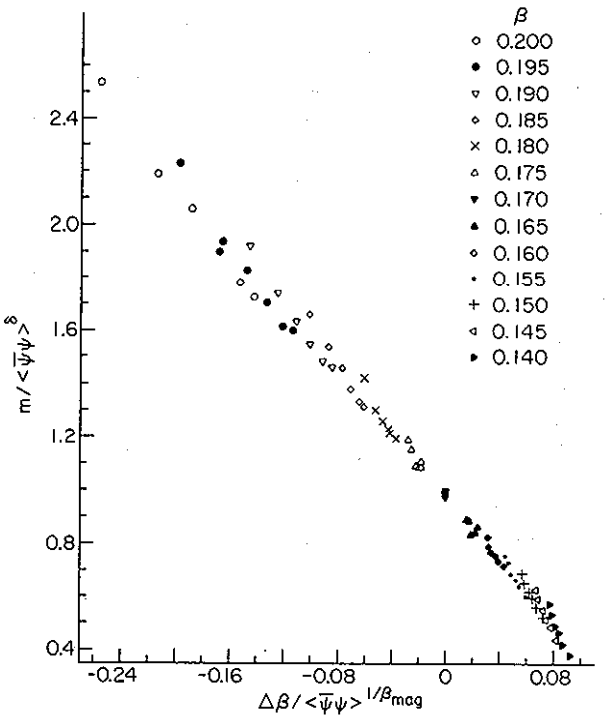

FIG. 2. Equation of state for $N_f = 8$ theory.

Next, we accumulated monopole percolation data for the $N_f = 8$ theory on a 10^4 lattice at various m. The data for χ, the monopole susceptibility, and M, the monopole percolation order parameter, are presented in Table V.

TABLE V. Monopole data, $N_f = 8, L = 10$.

	$m = 0.03$		$m = 0.04$		$m = 0.05$		$m = 0.06$		$m = 0.10$	
β	χ	M	χ	M	χ	M	χ	M	χ	M
0.20	19.75(16)	0.041(1)	21.98(22)	0.045(1)	23.45(32)	0.051(1)	25.15(27)	0.053(1)	34.69(56)	0.088(2)
0.195	24.1(2)	0.050(1)	26.48(30)	0.055(1)	28.55(30)	0.060(1)	30.89(46)	0.078(2)	45.4(9)	0.125(3)
0.19	30.9(4)	0.071(1)	34.00(50)	0.076(2)	36.44(52)	0.084(2)	40.35(61)	0.099(3)	51.6(1.5)	0.221(6)
0.185	39.7(7)	0.106(3)	41.58(74)	0.123(3)	48.4(.97)	0.137(4)	48.11(1.11)	0.180(5)	37.7(1.97)	0.383(6)
0.180	48.5(9)	0.152(4)	55.53(1.4)	0.180(4)	49.6(1.8)	0.266(6)	45.6(2.2)	0.330(6)	19.94(1.6)	0.535(5)
0.175	46.0(1.8)	0.298(6)	42.3(1.9)	0.351(6)	31.11(1.99)	0.434(6)	27.18(1.7)	0.473(6)	8.31(98)	0.652(3)
0.17	28.1(2.3)	0.457(6)	18.6(1.4)	0.519(5)	11.12(66)	0.586(3)	9.04(74)	0.623(3)	3.70(10)	0.747(2)
0.165	13.8(1.1)	0.579(4)	7.67(52)	0.649(3)	5.45(17)	0.692(2)	4.08(12)	0.727(2)	2.11(3)	0.810(1)
0.16	5.19(17)	0.709(2)	3.99(11)	0.736(2)	2.94(6)	0.772(2)	2.28(3)	0.798(1)	1.33(2)	0.859(1)
0.155	2.48(3)	0.789(1)	2.09(3)	0.809(1)	1.58(2)	0.837(1)	1.32(1)	0.855(1)	0.078(1)	0.899(1)
0.15	1.46(2)	0.848(1)	1.191(2)	0.867(1)	0.95(1)	0.883(1)	0.81(1)	0.895(1)	0.50(1)	0.9270(6)
0.145	0.082(1)	0.897(1)	0.69(1)	0.908(1)	0.55(1)	0.920(1)			0.032(1)	0.9483(4)
0.14	0.50(1)	0.927(1)	0.42(1)	0.937(1)	0.32(1)	0.946(1)			0.21(1)	0.9639(3)

We see that the peak of the susceptibility χ occurs at a coupling between 0.175 and 0.180 for $m = 0.03$, and it moves to slightly weaker coupling, 0.19, as m increases to 0.10. Our estimate of $\beta_c = 0.17$ for the chiral transition refers, of course, to the $m = 0$ chiral limit. So, within uncertainties because of finite size effects, the chiral and monopole percolation transitions are coincident, as we found with better numerical control for $N_f = 2$ and 4. There it was demonstrated that monopole susceptibility calculations can be done reliably at lower m values than $\ln\langle\bar{\psi}\psi\rangle$ calculations because the position of the peak in χ suffers from smaller finite size effects. It is important to determine if the peaks in χ on the 10^4 lattice are indicative of a real transition. To obtain some evidence for this result and to measure some critical indices, we repeated the measurements summarized in Table V on $10^4, 12^4, 14^4$, and 16^4 lattices at $m = 0.05$. The data are given in Table VI. We see that the peaks grow with L and they occur at a size-independent value of the coupling β. According to finite size scaling, the peak heights should grow as

$$\chi_{\max}(L) \sim L^{\gamma_{\rm mon}/\nu_{\rm mon}} \tag{2.4}$$

where $\gamma_{\rm mon}$ and $\nu_{\rm mon}$ are the susceptibility and correlation length exponents for the monopole transition. In addition, the order parameter at the coupling $\beta_{\max}$ where χ peaks for each L should scale to zero as

$$M[\beta_{\max}(L)] \sim L^{-\beta_{\rm mon}/\nu_{\rm mon}}. \tag{2.5}$$

We test these scaling predictions in Fig. 3 and find that the data supports power law scaling with the indices

$$\gamma_{\rm mon}/\nu_{\rm mon} = 2.25(3),$$
$$\beta_{\rm mon}/\nu_{\rm mon} = 0.875(80). \tag{2.6}$$

These are exactly the critical indices of ordinary four-dimensional percolation. Four-dimensional percolation indices satisfy hyperscaling relations and Eq. (2.5) then predicts $\nu_{\rm mon} = \frac{2}{3}$. This is the correlation length scaling index discussed in the introduction. Its coincidence with the correlation length exponent of the chiral transition is crucial to the monopole-percolation-driven chiral-transition physical picture.

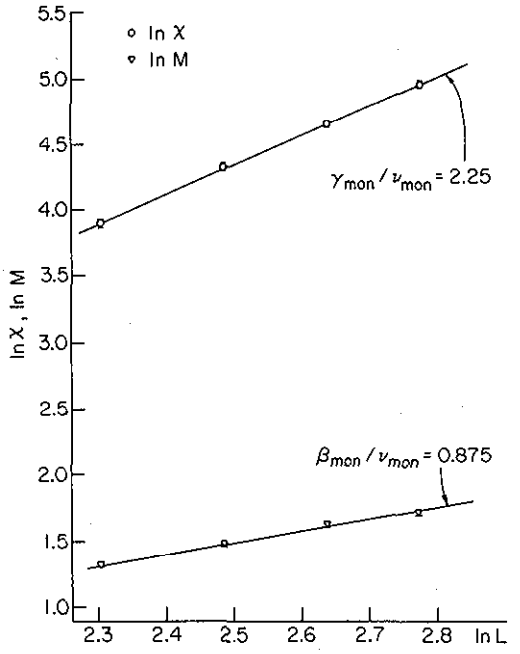

FIG. 3. Scaling plots, Eqs. (2.3) and (2.4), of monopole percolation quantities for $N_f = 8$ theory.

In summary, our 10^4 numerical results are compatible with the idea that the $N_f = 8$ chiral transition is physically indistinguishable from the $N_f = 2$ and 4 chiral transitions. If we assume power law critical singularities, then the physical picture of monopole percolation driving the chiral transition is also defensible because the couplings of the transitions coincide as do their correlation length indices.

III. MONOPOLE CONDENSATION AT $N_f = 24$

We next increased N_f in our hybrid Monte Carlo code and simulated the $N_f = 12, 16, 20$, and 24 models on 10^4 lattices with $m = 0.10$. A relatively large bare fermion mass was chosen to control finite size effects. The rela-

TABLE VI. Monopole observable scaling, $N_f = 8$.

β/L	10		12		14		16	
	χ	M	χ	M	χ	M	χ	M
0.20			25.8(3)	0.0267(2)				
0.19			48.0(6)	0.058(1)				
0.185			66(1)	0.105(3)	83(1)	0.076(2)	104(2)	0.061(1)
0.18	50(2)	0.266(6)	75(3)	0.228(5)	107(3)	0.197(4)	142(4)	0.180(3)
0.175			42(3)	0.409(4)	40(3)	0.415(4)	40(2)	0.412(2)
0.17			11.9(4)	0.575(2)				
0.16			2.89(4)	0.773(1)				
0.15			0.937(8)	0.886(1)				
0.14			0.359(4)	0.945(1)				

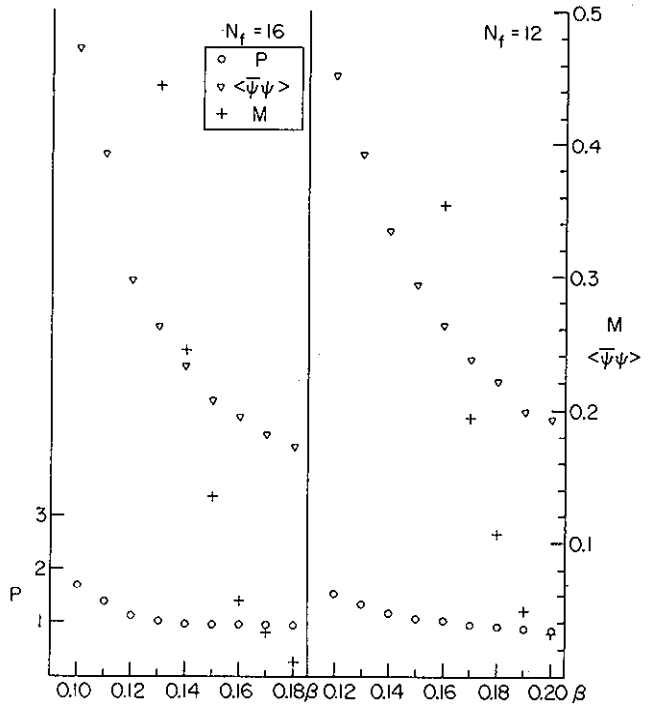

FIG. 4. Chiral condensate $\langle\bar{\psi}\psi\rangle$, monopole percolation order parameter M, and average plaquette P for $N_f = 12$ and 16 theories.

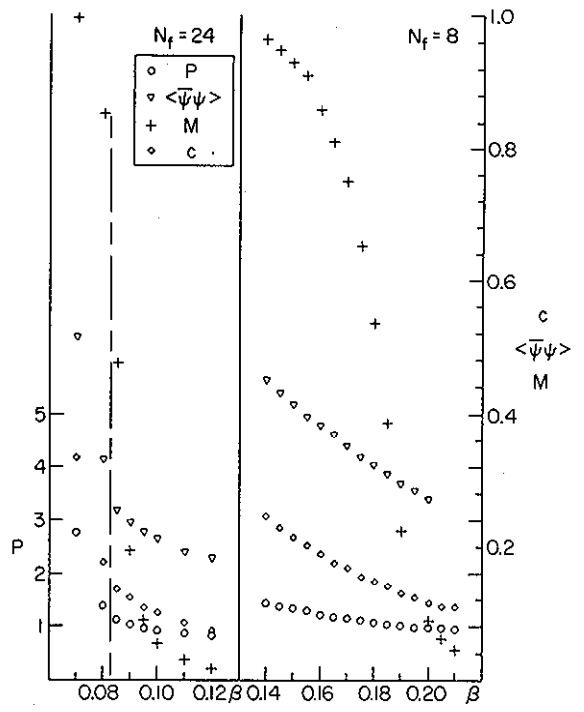

FIG. 6. Same as Fig. 4 except $N_f = 8$ and 24, but the monopole concentration c is shown as well.

tively large symmetry-breaking field will smooth out the chiral transition and make quantitative investigations impossible. However, qualitative changes in the dynamics of the model will be seen. The reader should understand, however, that we cannot predict the precise N_f values where qualitative changes occur. More simulations at smaller bare fermion masses on larger lattices will be needed for that.

The simulation data for the average plaquette P, the chiral condensate $\langle\bar{\psi}\psi\rangle$, and the monopole percolation order parameter M are shown in Fig. 4 for $N_f = 12$ and 16. The transition region between small $\langle\bar{\psi}\psi\rangle$ (or M), and

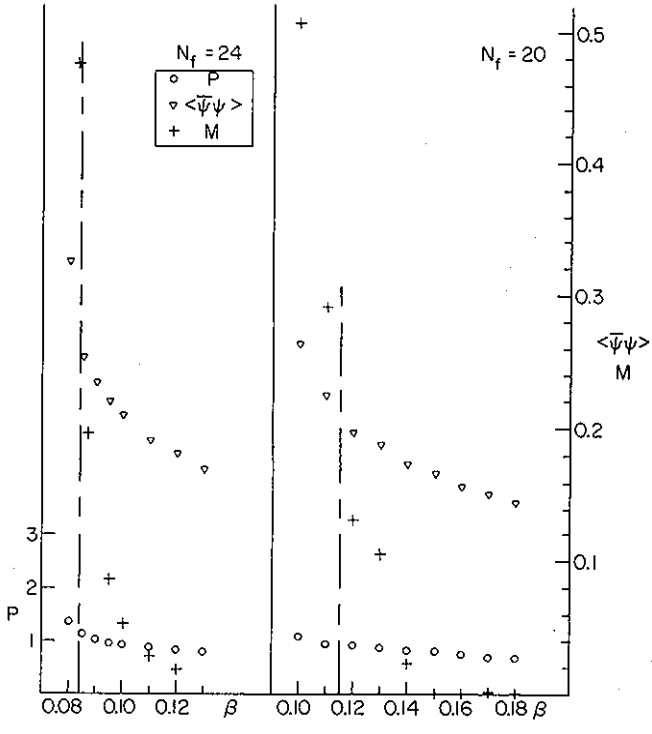

FIG. 5. Same as Fig. 4 except $N_f = 20$ and 24.

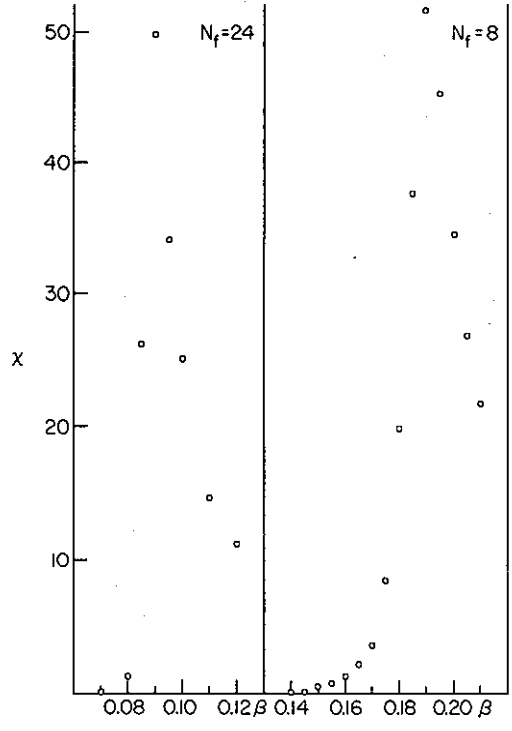

FIG. 7. Monopole percolation susceptibility plots for $N_f = 8$ and 24.

TABLE VII. $N_f = 8$ data.

β	P	$\langle\bar{\psi}\psi\rangle$	χ	M	c
0.21	0.961.(2)	0.2550(8)	21.9(2)	0.046(1)	0.1104(2)
0.205	0.972(2)	0.2643(8)	27.0(3)	0.060(1)	0.1093(2)
0.20	0.983(2)	0.2739(7)	34.7(6)	0.088(2)	0.1163(2)
0.195	0.993(2)	0.2835(7)	45.4(9)	0.125(3)	0.1232(2)
0.19	1.005(2)	0.2958(7)	52(2)	0.221(6)	0.1309(2)
0.185	1.023(2)	0.3098(8)	38(2)	0.383(6)	0.1396(3)
0.18	1.040(2)	0.3232(8)	20(2)	0.535(5)	0.1482(2)
0.175	1.110(2)	0.3364(9)	8.3(9)	0.652(3)	0.1573(2)
0.17	1.151(2)	0.352(1)	3.7(1)	0.747(2)	0.1682(2)
0.165	1.180(2)	0.369(1)	2.11(3)	0.810(1)	0.1791(2)
0.16	1.196(2)	0.382(1)	1.33(2)	0.859(1)	0.1900(2)
0.155	1.271(2)	0.399(1)	0.78(1)	0.899(1)	0.2033(2)
0.15	1.310(2)	0.417(1)	0.50(1)	0.9270(6)	0.2163(2)
0.145	1.372(2)	0.434(1)	0.32(1)	0.9483(4)	0.2299(2)
0.14	1.464(2)	0.452(1)	0.21(1)	0.9639(3)	0.2451(2)

large $\langle\bar{\psi}\psi\rangle$ (or M) shifts toward stronger coupling and the transition somewhat sharpens. The shift toward stronger coupling is a consequence of dynamical fermion screening and has been seen in many contexts before. In Fig. 5, we show the same plots for $N_f = 20$ and 24. Now there are suggestions that for each N_f, the order parameters $\langle\bar{\psi}\psi\rangle$ and M jump at the same coupling from smaller to larger values. This is particularly persuasive for $N_f = 24$ where we see signs of discontinuities at $\beta = 0.0825(25)$. Perhaps this qualitative effect is more visual in Fig. 6, where the $N_f = 24$ and $N_f = 8$ data for $m = 0.10$ are plotted and we have added the monopole concentration (density) "c" to the list of observables. The chiral condensate, monopole concentration, and average plaquette each appear to jump for $\beta = 0.0825(25)$. Certainly, for strong coupling, $\beta < 0.0825$, their slopes are much greater than their slopes at weak coupling, $\beta > 0.0825$. By contrast, the same set of observables are smooth in the plot of the $N_f = 8$ data. Of course, there is a transition in the $N_f = 8$ data, but it does not show up clearly at relatively large values of m, except in the monopole percolation observables M and χ. In fact, we plot the monopole percolation susceptibilities χ for the $N_f = 8$ and 24 theories at $m = 0.10$ in Fig. 7. Strong peaks are seen for both the N_f values with the width of the $N_f = 24$ peak considerably reduced, again indicating the relative sharpness of the $N_f = 24$ transitions.

Perhaps the clearest indication that the dynamics of the $N_f = 24$ model is qualitatively different from that

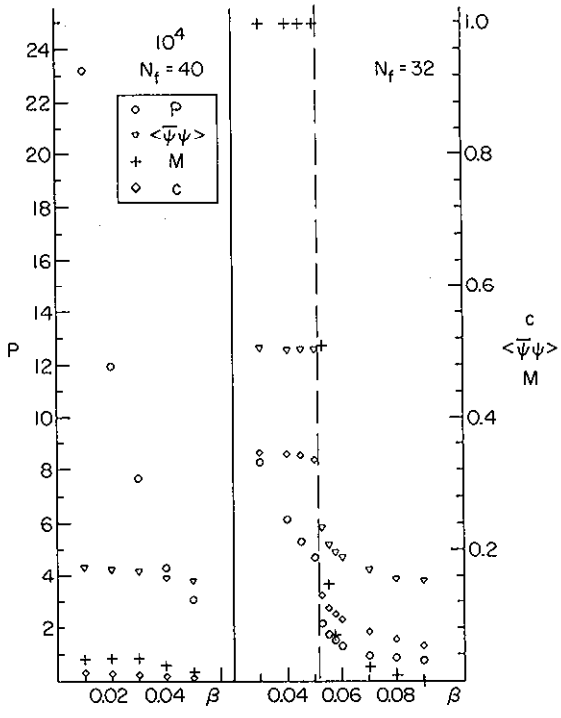

FIG. 8. Same as Fig. 6 except $N_f = 32$ and 40.

of the $N_f = 8$ case, comes from the monopole concentration. As seen in Tables VII and VIII, of $N_f = 8$ and $N_f = 24$ data at $m = 0.10$ on 10^4 lattices, the monopole concentration "jumps" in the $N_f = 24$ case while it is perfectly smooth through the percolation transition in the $N_f = 8$ case. This suggests that the monopoles are condensing in the $N_f = 24$ theory and the ground state for $\beta < 0.0825(25)$ is a monopole condensate, perhaps resembling the strong coupling, confining vacuum of the compact U(1) lattice QED model. Since the monopole concentration is small for $\beta > 0.0825(25)$ and jumps to a distinctly larger value for $\beta < 0.0825(25)$, we may be seeing signs of a first-order gas-liquid monopole condensation transition. Note that the percolation order parameter M and its susceptibility χ are near their kinematic extremes on the strong coupling side of the transition (at $\beta = 0.07$, say) and even the monopole concentration c is a substantial fraction of its extremal value (which is just under 1/2). These properties of M, χ, and c will be seen equally clearly in the $N_f = 32$ model which will be

TABLE VIII. $N_f = 24$ data.

β	P	$\langle\bar{\psi}\psi\rangle$	χ	M	c
0.12	0.799(1)	0.183(1)	11.2(1)	0.019(1)	0.0730(2)
0.11	0.845(1)	0.193(1)	14.8(2)	0.029(2)	0.0847(2)
0.10	0.915(1)	0.211(1)	25.1(3)	0.053(2)	0.1002(2)
0.095	0.955(1)	0.222(1)	34.2(7)	0.088(3)	0.1089(2)
0.09	1.019(1)	0.238(1)	50(2)	0.197(7)	0.1211(3)
0.085	1.097(1)	0.258(1)	26(3)	0.476(7)	0.1356(3)
0.08	1.336(2)	0.329(1)	1.36(3)	0.853(2)	0.1794(5)
0.07	2.77(1)	0.516(2)	0.0076(5)	0.9983(2)	0.3354(8)

TABLE IX. $N_f = 32$ data.

β	P	$\langle\bar{\psi}\psi\rangle$	χ	M	c
0.09	0.7366(6)	0.1524(4)	8.29(4)	0.0024(6)	0.052(1)
0.08	0.8100(7)	0.1586(4)	9.68(5)	0.0102(9)	0.061(1)
0.07	0.934(1)	0.1687(5)	11.90(8)	0.0218(9)	0.073(1)
0.06	1.276(2)	0.1867(6)	20.2(3)	0.045(1)	0.092(1)
0.0575	1.509(2)	0.1954(9)	29.2(9)	0.061(4)	0.100(1)
0.055	1.692(1)	0.2070(7)	41.7(9)	0.146(6)	0.110(1)
0.0525	2.151(1)	0.2339(7)	17.4(9)	0.509(6)	0.130(1)
0.05	4.639(4)	0.509(1)	0.0048(2)	0.9989(1)	0.335(1)
0.045	5.315(4)	0.516(2)	0.0047(2)	0.9989(1)	0.342(1)
0.04	6.127(2)	0.513(2)	0.0048(2)	0.9989(1)	0.343(1)
0.03	8.305(5)	0.517(1)	0.0045(2)	0.9989(1)	0.344(1)

discussed further below. The monopole activation energy is proportional to $\frac{1}{e^2} = \beta$ and it is relatively small here compared to the small N_f models. As the coupling is increased through 0.0825(25), a first-order monopole condensation transition into a monopole liquid is triggered where a relatively dense monopole ensemble is produced. It would be interesting to study the monopole dynamics through correlation functions in this condensed state and compare them to similar simulations in pure compact QED.

IV. MONOPOLE AND CHIRAL SUPPRESSION AT $N_f = 40$

In this survey of N_f, we next turned to the $N_f = 32$ model. The data is presented in Table IX (for $m = 0.10$ and 10^4 lattices, as usual) and it is plotted in Fig. 8. Jumps are seen in all observables for $N_f = 32$ at a coupling $\beta = 0.05125(125)$. On the strong coupling side of the transition, $M, \langle\bar{\psi}\psi\rangle$, and c are saturated. The average plaquette has also jumped at $\beta = 0.05125(125)$, and is growing rapidly in the strong coupling phase. A first-order monopole condensation transiton is very apparent.

We finally increased N_f to 40 in order to see the effects of extreme fermion screening. Table X and Fig. 8 resulted—the monopole and chiral observables are almost completely suppressed. Throughout the entire range of couplings $\langle\bar{\psi}\psi\rangle$ remains near its weak coupling value. Both of the percolation observables, χ and M, are strongly suppressed and are slightly smaller at $\beta = 0.01$ than those at $\beta = 0.02$. The average plaquette P rapidly increases over this range of β, however, probably indicative of a persistent specific heat anomaly, as discussed more quantitatively by Azcoiti and collaborators [10]. Our interest in this result is again the strong correlation between the monopole and chiral observables. The fact that they are both deeply suppressed, even while the average plaquette indicates considerable "disorder" in the ground state, is supportive of the physical picture which contends that the effective monopoles are essential in the model's chiral dynamics at all N_f.

V. CONCLUDING REMARKS

In this survey of N_f, we have found that chiral and monopole dynamics are strongly correlated in every case.

A. Small N_f

The monopole transition is a second-order percolation transition without condensation. If the chiral transition is assumed to be characterized by power law singularities, satisfying hyperscaling, then it was coincident with monopole percolation and the correlation length indices of the two transitions were identical.

B. Intermediate N_f

The monopole transition becomes a first-order condensation phenomenon. The chiral transition is coincident and also first-order.

TABLE X. $N_f = 40$ data.

β	P	$\langle\bar{\psi}\psi\rangle$	χ	m	c
0.05	3.042(4)	0.1522(5)	10.6(1)	0.012(1)	0.063(1)
0.04	4.275(4)	0.1567(4)	11.9(1)	0.024(1)	0.069(1)
0.03	7.648(5)	0.1672(4)	15.2(2)	0.036(1)	0.075(1)
0.02	11.956(6)	0.1686(5)	15.9(2)	0.037(1)	0.089(1)
0.01	23.207(7)	0.1692(5)	15.5(2)	0.034(1)	0.111(2)

C. Large N_f

The monopole and chiral observables are strongly suppressed, and there is no transition in any of these quantities. The average plaquette is rapidly varying as a function of coupling nonetheless.

In summary, it may be worthwhile to pursue in more detail some aspects of the dynamics found here. The nature of the chiral transition for small N_f is a primary goal, since it may define an interacting field theory which is strongly coupled at short distances. The nature of the field theory and the role of effective monopoles in it would be interesting to understand. The monopole condensate at intermediate N_f and its "liquid" properties would be interesting to clarify through correlation functions.

ACKNOWLEDGMENTS

J.B.K. is supported in part by the National Science Foundation, Grant No. NSF PHY92-00148. The computer simulations described here were done on the C90's at NERSC and PSC. The authors thank the staffs of these facilities for their expertise. J.B.K. thanks M.-P. Lombardo for helping with several of the fits which used CERNLIB and MINUIT.

[1] C. Callan, Phys. Rev. D **26**, 2058 (1982); V. A. Rubakov, Nucl. Phys. **B203**, 311 (1982).
[2] T. Banks, R. Myerson, and J. Kogut, Nucl. Phys. **B129**, 493 (1977).
[3] S. Hands and R. Wensley, Phys. Rev. Lett. **63**, 2169 (1989).
[4] S. Hands, A. Kocic, and J. Kogut, Phys. Lett. B **289**, 400 (1992).
[5] S. Hands, A. Kocic, J. Kogut, R. Renken, D. K. Sinclair, and K. C. Wang, Nucl. Phys. **B413**, 503 (1994); A. Kocic, J. Kogut, and K. C. Wang, *ibid.* **B398**, 405 (1993).
[6] A dissenting view is offered by M. Gockeler *et al.*, Nucl. Phys. **B371**, 713 (1992).
[7] T.A. DeGrand and D. Toussaint, Phys. Rev. D **22**, 2478 (1980).
[8] S. Hands and J. Kogut, in *Lattice '94*, Proceedings of the International Symposium, Bielefeld, Germany, edited by F. Karsch *et al.* [Nucl. Phys. **B** (Proc. Suppl. **42**, 663 (1995)]; Nucl. Phys. **B371**, 713 (1992).
[9] E. Dagotto, A. Kocic, and J. Kogut, Phys. Lett. B **232**, 235 (1989).
[10] V. Azcoiti, G. Di Carlo, and A. F. Grillo, Phys. Lett. B **305**, 275 (1993).